

# Measurement and correlation of hydraulic resistance of flow through woven metal screens

W.T. Wu, J.F. Liu, W.J. Li, W.H. Hsieh \*

*Department of Mechanical Engineering, National Chung Cheng University, Chia-Yi 621, Taiwan, ROC*

Received 6 April 2004

Available online 9 April 2005

## Abstract

In this study, an experimental setup was established to measure the pressure drop of flow through woven metal screens. Four woven metal screens with different porosities of the plain-square type were tested in this study. The Reynolds number based on the equivalent spherical diameter of the metal screen ranged from low  $Re$  ( $Re = 85$ ) to high  $Re$  ( $Re = 12000$ ). The range of porosity was 0.834–0.919. Based on the measured pressure drops of the four woven metal screens, this study developed an empirical equation of friction characteristic of plain-square-type woven metal screens. All experimental data for the plain-square-type screens lie within  $\pm 30\%$  of the empirical equation. Based on the fact that the measured pressure drops of single-layer and multiple-layer woven metal screens can all be fit into a single equation, it is noted that the velocity developing region is very short for woven metal screens. In order to obtain good agreement between the fitted empirical equation and measured data, this study noted that an empirical equation should be developed for each type of the woven metal screen. This study developed five empirical equations respectively for the five types of metal screens, (plain square, plain dutch, fourdrinier, full twill, and twilled dutch types) of which experimental data were available in open literature and the present study.

© 2005 Elsevier Ltd. All rights reserved.

*Keywords:* Porous media; Woven metal screens; Pressure drops; Transport properties

## 1. Introduction

The augmented heat- and mass-transfer characteristics of porous media have led to numerous applications. Kays and London [1] pointed out that an effective way to increase the performance of a heat exchanger is to increase its surface area to volume ratio. Open cell porous

matrix such as an unconsolidated bed of small particles, woven metal screens, or foam matrixes provides excellent heat-transfer characteristics due to its large surface area to volume ratio. Therefore, woven metal screens have been used in solar-receiving devices [2], high-efficiency heat exchangers [1], energy-storage units [1], regenerators in Stirling cryocoolers [3], electronic coolers [4,5], catalytic reactors [6], and others. In filtering industry, woven metal screens are also widely used in the filtering of fluids due to their good resistance to chemical, thermal, and mechanical influences in comparison with textile and paper made filters. Other advantages of woven metal screens include easy arrangement,

\* Corresponding author. Tel.: +886 5 2428170; fax: +886 5 2720589.

*E-mail address:* [imewhh@ccunix.ccu.edu.tw](mailto:imewhh@ccunix.ccu.edu.tw) (W.H. Hsieh).

**Nomenclature**

$D_P$	equivalent spherical diameter of porous media
$f_k$	friction factor, defined in Eq. (1)
$L$	length of the test section
$P$	pressure
$Re$	Reynolds number based on the equivalent spherical diameter of porous media

$S_v$	surface area per unit volume of solid phase
$U$	velocity of the fluid

*Greek symbols*

$\rho$	density
$\mu$	viscosity
$\varepsilon$	porosity

high permeability and relatively small deviation of the pore size from the mean value.

Although woven metal screens offer the aforementioned merits, information on hydraulic resistance of woven metal screens is required when using these types of materials in any systems. Woven metal screens are usually classified by weaving types; there are four common types: the plain weaves, twill weaves, fourdrinier weaves, and dutch weaves. Plain weaves: This is the most popular wire cloths weave. Each weft wire passes alternately over and under each warp wire and each warp wire passes alternately over and under each weft wire. Warp and weft wire diameters are generally the same. Twill weaves: Each weft wire alternately passes over two, then under two successive warp wires and each warp wire passes alternately over two and under two successive weft wires, in a staggered arrangement. Fourdrinier weaves: This kind of weave is a mixture of plain and twill weaves and is also called semi-twill weaves. Dutch weaves: The warp wires remain straight; the weft wires are woven to lie as close as possible against each other in a linen weave forming a dense strong material with small, irregular and twisting passageways that appear triangular when diagonally viewing the weave. The schematic diagram of these four types of woven metal screens is shown in Fig. 1.

In 1964, Kays and London [1] presented the measured friction factor of four woven metal screens (plain square type). Armour and Cannon [7] investigated the hydraulic resistance of five types (plain square, fourdrinier, full twill, plain dutch, and twilled dutch types) of woven metal screens through experiments made in a round channel with only a single layer of metal screen. They provided an equation for the calculation of pressure drop based on the flow velocity, the porosity, and the geometry of the screen. Sodré and Parise [8] designed an experimental procedure to investigate the friction factor of the plain-square woven metal screen adopted in the Stirling engine regenerator. They developed an equation to evaluate the pressure drop in the annular bed of screens.

Though many studies were devoted to analyzing the pressure drop through woven screen matrices, there is

still a need to find out if there is a general empirical equation suitable for various types of woven metal screens. In this study, a series of experimental tests was conducted to determine the flow friction characteristic of woven metal screens. Four woven metal screens (plain square type) with different porosities were tested. A general empirical equation was developed to correlate the dimensionless pressure drop ( $f_k$ ) and flow velocity ( $Re$ ) for the four woven metal screens and the empirical equation is extended to high  $Re$  region. Comparison of the empirical correlation with experimental data in open literature validated the empirical correlation. Following the form of the correlation developed in this study, an empirical correlation is also developed for each one of the other four types of metal screens (plain dutch, fourdrinier, full twill, and twilled dutch types).

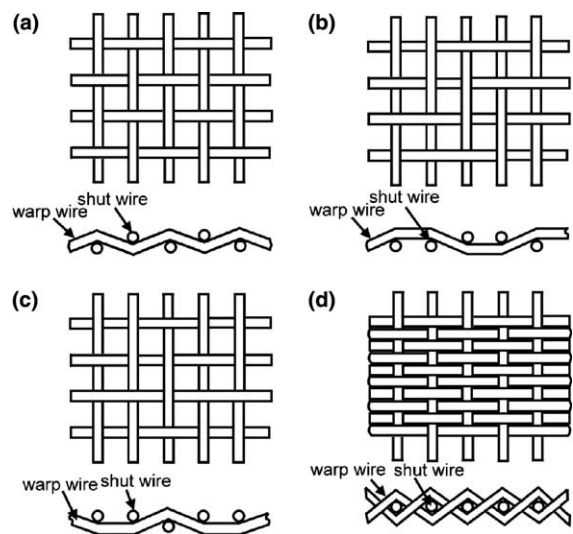


Fig. 1. Schematic diagram of four common types of woven metal screens: (a) plain weaves, (b) twill weaves, (c) fourdrinier weaves, and (d) dutch weaves.

## 2. Experimental approach

### 2.1. Apparatus

A sketch of the experiment setup used for the measurement of the pressure drop through woven metal screens is shown in Fig. 2. A compressor supplied air for the whole system. The compressed air was first stored in a surge tank, and then it went through a filter and a dehydrator in series to remove suspended particles, water, and oil before entering the test section. A plenum chamber was used to stabilize the pressure in the test setup. The plenum chamber was equipped with a needle valve to fine-tune the flow rate of air. The volumetric flow rate of the air was measured with a turbine flow meter (EG&G, 0.3% accuracy). On the downstream of the turbine flow meter, the pressure and temperature were monitored, respectively, using a Validyne pressure transducer (0.5% accuracy) and a thermocouple (T-type thermocouple, calibrated to within 80 °C, 0.75% accuracy) for further determination of the air density.

The up- and down-streams of the test section were both equipped with honeycomb straighteners for unifying the flow field. The test section was 20 cm in length and 6.5 cm in diameter to reduce the entrance and wall effects [11]. The entrance and the exit of the test section were both installed with Validyne pressure transducers (0.5% accuracy) to measure pressure drops. Experimental data were taken by a Fluke Hydra series portable data acquisition system with a frequency of 100 Hz. Data were transferred to a computer through a RS-232 interface.

Before each experiment, thermocouples and pressure transducers were calibrated. The pipeline was tested for leakage to ensure the accuracy of the measurements of

flowrate. During a test, experimental data were recorded for at least 20 min to ensure that a steady-state condition was achieved. Each experimental condition was repeated for at least 5 times. Average data of the repeated experiments were used for analysis.

### 2.2. Geometry of woven metal screens

Present study adopted AISI 304 metal screens woven in plain square type. Fig. 3 shows the sketch of the metal screen. The  $d_w$  and  $d_s$  are the wire diameters of the warp wire and the shut wire, respectively. The average wire diameters and distance between wires are determined by averaging ten randomly measured data by an optical microscope. Metal screens cut into a circular shape with a diameter of 6.5 cm are packed layer by layer in the 20 cm long test section.

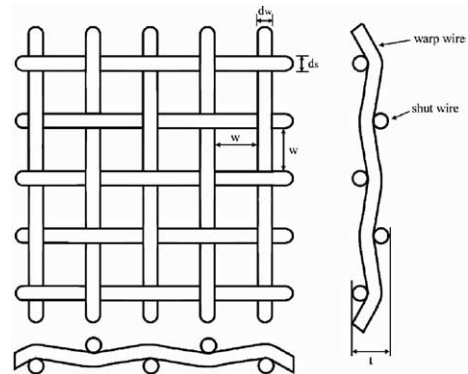


Fig. 3. Schematic diagram of metal screen woven in plain square type.

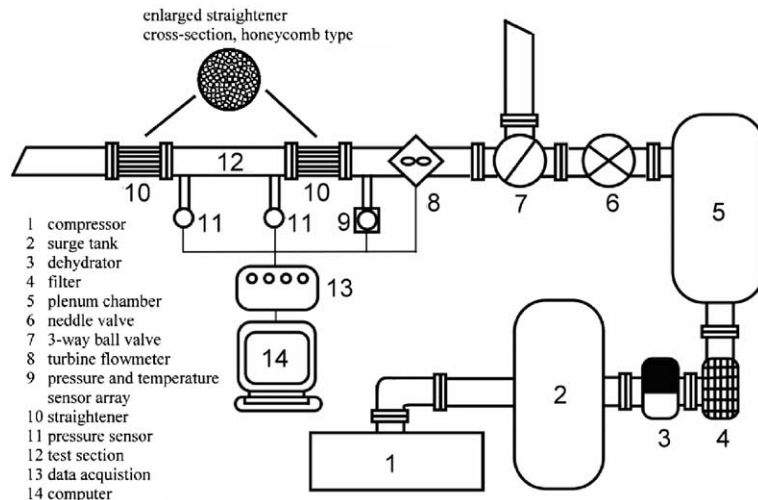


Fig. 2. Schematic diagram of screen flow apparatus.

Table 1  
Properties of AISI 304 metal screens

Woven type	Plain square type			
Porosity	0.919	0.876	0.866	0.834
Diameter of screen (m)	$6.5 \times 10^{-2}$	$6.5 \times 10^{-2}$	$6.5 \times 10^{-2}$	$6.5 \times 10^{-2}$
Mass of a single screen (kg)	$3.7 \times 10^{-3}$	$2.9 \times 10^{-3}$	$1.9 \times 10^{-3}$	$2.2 \times 10^{-3}$
Thickness of a single screen (m)	$1.7 \times 10^{-3}$	$9.0 \times 10^{-4}$	$5.4 \times 10^{-4}$	$5.0 \times 10^{-4}$
Diameter of warp wire (m)	$5.1 \times 10^{-4}$	$3.0 \times 10^{-4}$	$2.3 \times 10^{-4}$	$2.0 \times 10^{-4}$
$D_P$ (m)	$1.33 \times 10^{-3}$	$7.26 \times 10^{-4}$	$4.15 \times 10^{-4}$	$3.90 \times 10^{-4}$
Woven density (wires/in.)	4	10	17	31

Table 1 shows the geometric parameters of the metal screens used in this study. The equivalent spherical diameter ( $D_P$ ), the characteristic length, of woven metal screens shown in Table 1 is defined as  $D_P = 6/S_v$ , where  $S_v$  is the surface area per unit volume of solid phase.

The surface area is calculated from the optically measured wire diameter and the distance between wires with the assumption of point-contact between wires. The volume of the solid metal is determined from the measured weight of the screen and the density of the metal.

### 2.3. Correlation of pressure-drop characteristics

Generally speaking, there are two major theoretical approaches for studying pressure drops of flows through porous materials. One approach is to treat a porous material as a bundle of tangled tubes; the theory is developed by applying flow friction characteristics for single straight tubes to the collection of crooked tubes. The second approach is to calculate the pressure drop by summing up the resistances of the submerged particles. In 1952, Ergun [9] successfully formulated a general equation to describe the pressure-drop characteristic of various types of granular porous materials according to tube-bundle theories. According to the characteristics of porous materials, such as closeness, orientation of packing, size, shape, and surface of particles, Ergun [9] introduced the modified fanning friction factor (the ratio of the wall shear stress at pipe/conduit to the flow kinetic energy) and the modified Reynolds number as

$$f_k = \frac{\Delta P}{L} \frac{D_P}{\rho U^2} \frac{\varepsilon^3}{1 - \varepsilon} \quad (1)$$

$$\frac{Re}{1 - \varepsilon} = \frac{D_P \rho U}{\mu} \quad (2)$$

The characteristic length in this equation is the equivalent spherical diameter ( $D_P$ ) of a porous media. Based on the modified fanning friction factor and the modified Reynolds number defined in Eqs. (1) and (2), Ergun [9] fitted the measured pressure-drop data of fluid flowing through granular porous materials into an equation given as below.

$$f_k = 150 \frac{1 - \varepsilon}{Re} + 1.75 \quad (3)$$

Based on Eq. (3), the pressure drop through a porous material is attributed to both viscous (the first term on the right hand side) and kinetic (the second term on the right hand side) losses. In determining the pressure-drop characteristics at high Reynolds number, Jones et al. [10] used high-pressure air as the flow source. They analyzed the pressure-drop characteristics of granular porous materials at high Reynolds numbers and modified the Ergun's equation (Eq. (3)) to include the high-Reynolds-number effect (the second term on the right hand side of Eq. (4)). The equation is given below.

$$f_k = 150 \frac{1 - \varepsilon}{Re} + 3.89 \left( \frac{1 - \varepsilon}{Re} \right)^{0.13} \quad (4)$$

The objectives of the present study are to understand better the pressure-drop characteristics of woven metal screens and to develop a general equation of pressure drop at an extended range of Reynolds number. This study, therefore, adopts a general equation, in the form of Eq. (4), given below in Eq. (5). A series of experiments were conducted to determine the coefficients  $\alpha$ ,  $\beta$ , and  $\gamma$  of Eq. (5).

$$f_k = \alpha \frac{1 - \varepsilon}{Re} + \beta \left( \frac{1 - \varepsilon}{Re} \right)^\gamma \quad (5)$$

## 3. Results and discussion

### 3.1. Empirical equation for pressure-drop characteristic of flow through woven metal screens

The modified fanning friction factors  $f_k$  of the four metal screens used in this study were determined following the definition given in Eq. (1) and plotted as functions of  $Re/(1 - \varepsilon)$  in Fig. 4. The uncertainties of  $f_k$  and  $Re$  are  $\pm 4.8\%$  and  $\pm 1.3\%$ , respectively, determined by the methods suggested by Benedict [12] and Kline et al. [13]. In Fig. 4, it is noted that  $f_k$  decreases with the increase of  $Re/(1 - \varepsilon)$ . It should also be noted that the data for the four woven metal screens fell well into

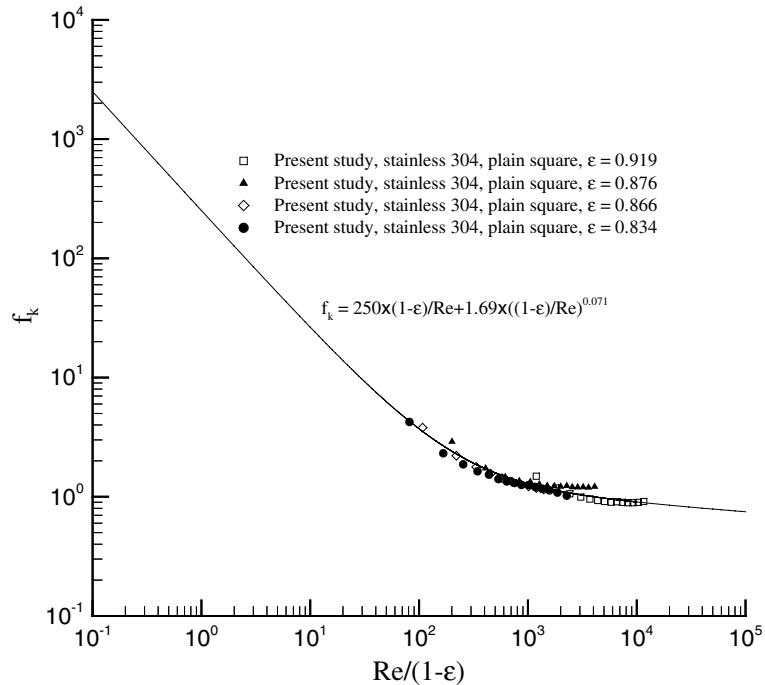


Fig. 4. Correlation between  $f_k$  and  $Re/(1 - \epsilon)$ .

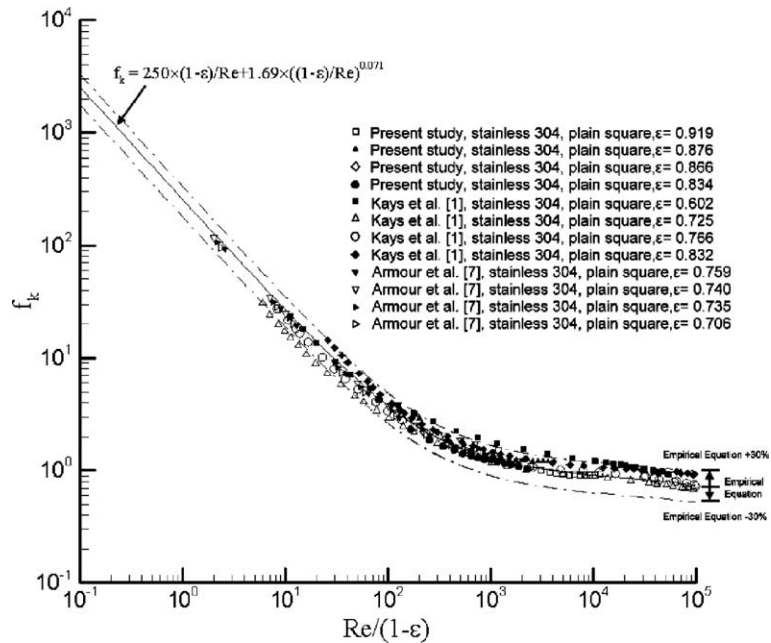


Fig. 5. Correlation between  $f_k$  and  $Re/(1 - \epsilon)$  for plain square type.

a single curve. Though many studies of friction characteristic of woven metal screens have been conducted before [7], this is the first time that a general correlation is

extended to the high Reynolds number regime. As shown in Fig. 4, the correlation for the four woven metal screens was determined to be

$$f_k = 250 \frac{1 - \varepsilon}{Re} + 1.69 \left( \frac{1 - \varepsilon}{Re} \right)^{0.071} \quad (6)$$

3.2. Comparison of correlation with related literature

In order to test the applicability of Eq. (6) developed in this work, Eq. (6) is compared with the experimental data of Kays and London [1] and Armour and Cannon [7]. Kays and London [1] adopted stainless steel screens of the plain square type, and the range of porosity was 0.602–0.832. They measured pressure drops of air flowing through randomly packed screens. Their test apparatus was similar to the present study. Their test section was made of a round pipe with an inner diameter of 7.6 cm. Armour and Cannon [7] also adopted stainless steel screens. They adopted five different types of woven screens, namely the plain square, full twill, fourdrinier, plain dutch, and twilled dutch type. The range of porosity was 0.35–0.759. The working fluids were nitrogen and helium, and they only measured pressure drops induced by a single layer of the screen.

Fig. 5 shows the comparison of Eq. (6) with the experimental data of the metal screens of the plain-square type from Refs. [1,7]. Fig. 5 shows that data from Refs. [1,7] and the present study all fall within ±30% of Eq. (6). Table 2 shows the range of modified Reynolds number  $Re/(1 - \varepsilon)$  in Fig. 5. The modified Reynolds number ranges between 0.5 and 98500, which covers from the laminar to turbulent regimes. Ref. [7] adopted

Table 2

Range of modified Reynolds number for metal screens of plain square type

Source	Range of modified Reynolds number	Layer
[1]	$0.5 < \frac{Re}{1 - \varepsilon} < 1300$	Single-layer
[7]	$6 < \frac{Re}{1 - \varepsilon} < 98500$	Multi-layer
Present study	$85 < \frac{Re}{1 - \varepsilon} < 12000$	Multi-layer

only a single layer of screen during tests, and the data from Ref. [7] is found to be well fitted by Eq. (6). This indicates that the flow developing region is very short and within the thickness of one layer of metal screens.

In order to examine the universality of Eq. (5), all experimental data for different types of metal screens from the present study and Refs. [1,7] are fit into a single equation in the form of Eq. (5). The fitted equation is given below.

$$f_k = 138 \frac{1 - \varepsilon}{Re} + 1.95 \left( \frac{1 - \varepsilon}{Re} \right)^{0.071} \quad (7)$$

Fig. 6 shows the comparison of Eq. (7) with experimental data. In Fig. 6, the solid line represents Eq. (7) and dash lines represent ±30% of Eq. (7), which are taken as the upper and lower bounds. (In the empirical correlations for granular beds [9] and foam matrixes [14], the deviations between experimental data and the correlations are all within ±30%.) There are more than

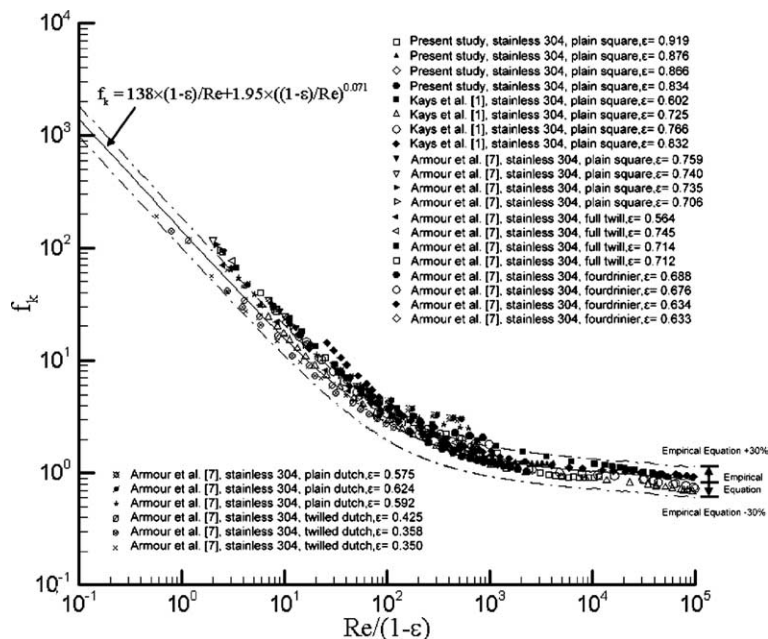


Fig. 6. Comparison of Eq. (7) with data of Refs. [1,7].

42% of experimental data lie at the outside of these bounds. It appears that a single equation fails to represent pressure-drop characteristics of flow through different types of metal screens. There should be different pressure-drop correlations for different types of metal screens.

### 3.3. Correlations for different types of metal screens

Fig. 7 shows correlations, in the form of Eq. (5), between  $f_k$  and  $Re/(1 - \epsilon)$  for the plain dutch and fourdrinier types. The correlation is obtained by fitting the experimental data form Ref. [7]. Fig. 7 shows that corre-

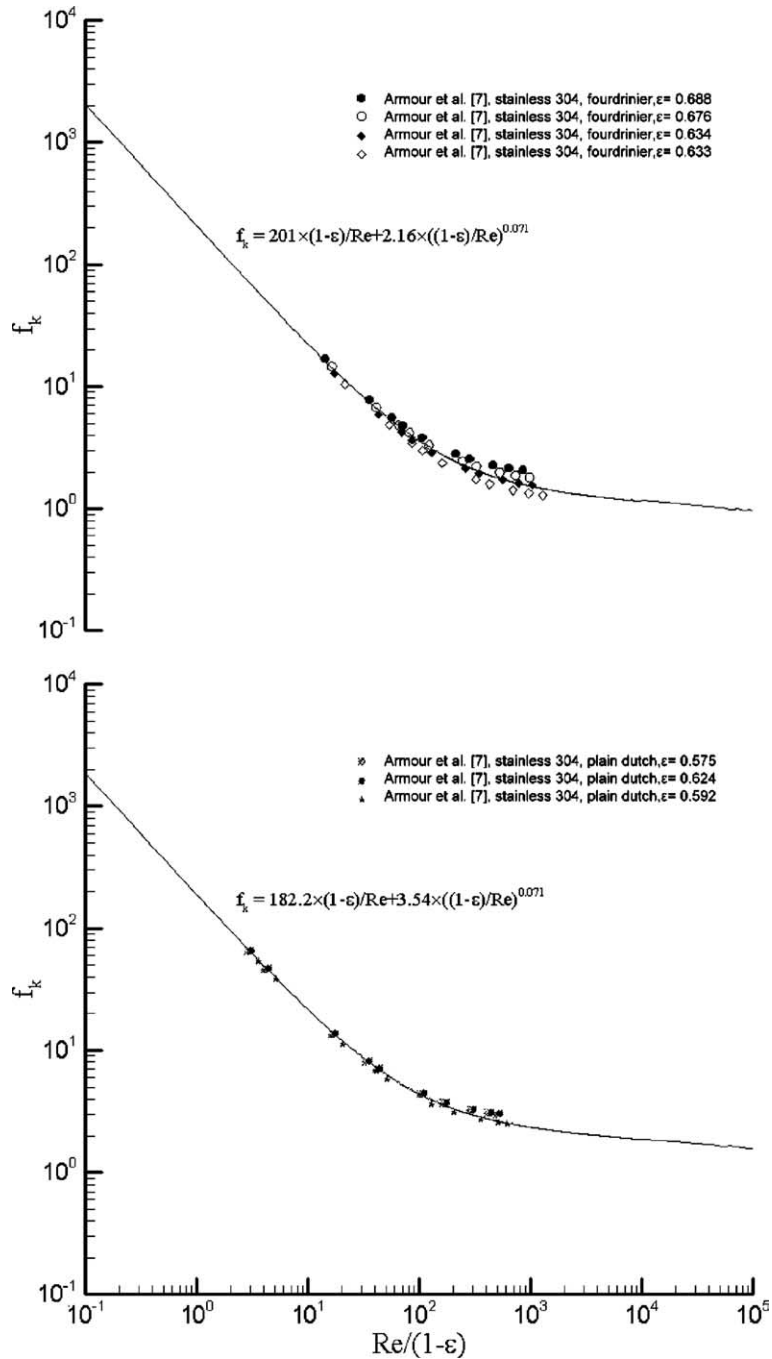


Fig. 7. Correlations between  $f_k$  and  $Re/(1 - \epsilon)$  for plain dutch and fourdrinier type.

lations fit experimental data very well. Fig. 8 shows correlations between  $f_k$  and  $Re/(1 - \epsilon)$  for the full twill and twilled dutch types. Fig. 8 shows that correlations fit experimental data [7] very well. Table 3 lists the coefficients of these correlations. Table 4 lists the woven type,

woven density, porosity, and equivalent spherical diameters of different woven type adopted in the present study and Ref. [7]. It should be noted that the coefficient,  $\gamma$ , is taken to be the same as that for the metal screens of the plain square type, due to the fact that the experimental

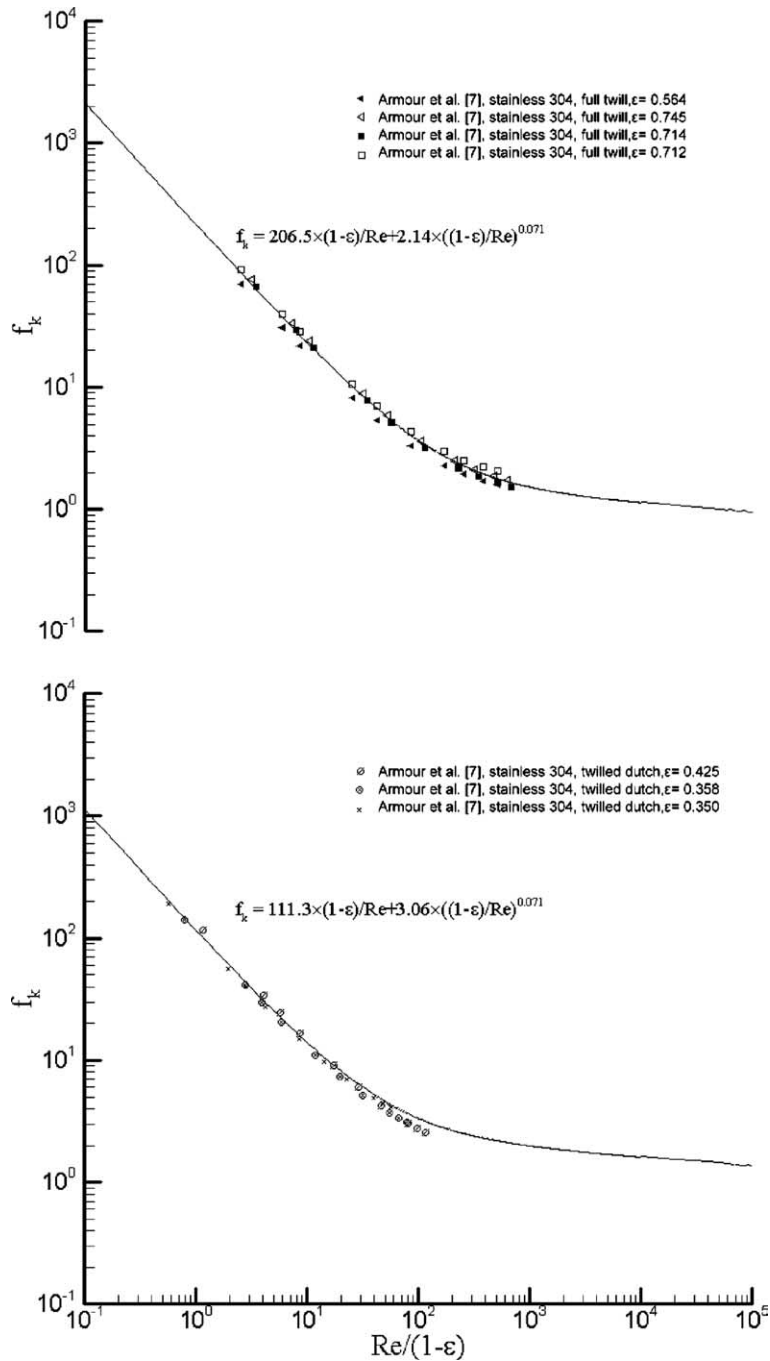


Fig. 8. Correlation between  $f_k$  and  $Re/(1 - \epsilon)$  for twilled dutch type and full twill type.



Table 3  
Coefficients of correlations<sup>a</sup>

Woven type	$\alpha$	$\beta$	$\gamma$
Plain square type	250	1.69	0.071
Plain dutch type	182.2	3.54	0.071
Fourdrinier type	201	2.16	0.071
Full twill type	206.5	2.14	0.071
Twilled dutch type	111.3	3.06	0.071

$$^a f_k = \alpha \frac{1-\varepsilon}{Re} + \beta \left( \frac{1-\varepsilon}{Re} \right)^\gamma.$$

Table 4  
Equivalent spherical diameters of porous media of screens of different woven type

Woven type	Woven density (wires/in.)	Porosity	$D_p$ (m)	Source
Plain square	4 × 4	0.919	$1.33 \times 10^{-3}$	Present study
	10 × 10	0.876	$7.26 \times 10^{-4}$	
	17 × 17	0.866	$4.15 \times 10^{-4}$	
	31 × 31	0.834	$3.90 \times 10^{-4}$	
	31 × 31	0.759	$1.54 \times 10^{-3}$	
	151 × 151	0.740	$3.72 \times 10^{-4}$	
Fill twill	248 × 248	0.735	$2.03 \times 10^{-4}$	[7]
	387 × 387	0.706	$1.17 \times 10^{-4}$	
	68 × 77	0.564	$6.76 \times 10^{-4}$	
	142 × 142	0.745	$3.44 \times 10^{-4}$	
Fourdriner	297 × 297	0.714	$1.94 \times 10^{-4}$	[7]
	406 × 406	0.712	$1.65 \times 10^{-4}$	
	55 × 32	0.688	$1.55 \times 10^{-3}$	
	63 × 43	0.676	$1.18 \times 10^{-3}$	
Plain dutch	76 × 60	0.634	$8.13 \times 10^{-4}$	[7]
	79 × 62	0.633	$6.46 \times 10^{-4}$	
	24 × 113	0.575	$9.08 \times 10^{-4}$	
Twilled dutch	30 × 152	0.624	$7.08 \times 10^{-4}$	[7]
	51 × 257	0.592	$3.96 \times 10^{-4}$	
	80 × 736	0.425	$2.05 \times 10^{-4}$	
	197 × 1499	0.358	$9.14 \times 10^{-5}$	[7]
	321 × 2105	0.350	$6.32 \times 10^{-5}$	

data at high modified Reynolds number  $Re/(1-\varepsilon)$  is available only for the metal screens of the plain square type.

#### 4. Summary and conclusions

In this work, an experimental setup was established to measure the pressure drop of flow through woven metal screens. Based on the measured pressure drops of four woven metal screens (plain square type), this study developed an empirical equation of friction characteristic for plain-square-type metal screens. The empirical equation is

$$f_k = 250 \frac{1-\varepsilon}{Re} + 1.69 \left( \frac{1-\varepsilon}{Re} \right)^{0.071}$$

where

$$f_k = \frac{\Delta P}{L} \frac{D_p}{\rho U^2} \frac{\varepsilon^3}{1-\varepsilon}, \quad \frac{Re}{1-\varepsilon} = \frac{D_p \rho U}{\mu}, \quad \text{and} \quad D_p = \frac{6}{S_v}$$

The empirical equation takes into account of the high Reynolds number effect by the second term on the right hand side of the equation and was developed based on the measured pressure drops of woven metal screens with the porosity ranging from 0.602 to 0.919 and the Reynolds number, 85 to 12000. Based on the fact that the pressure drop data of the single-layer [7] and multi-layer [present study and 1] screens can be fitted well by a single empirical correlation, it is noted that the flow developing region is very short, less than the thickness of a single layer of the metal screen. This study also suggested an empirical equation should be developed for each type of the woven metal screen, so that good agreement between the empirical equation and experimental data could be obtained.

#### Acknowledgement

This work represents a part of the results obtained under contract no. NSC-89-2212-E-194-023 sponsored by National Science Council, Taiwan, ROC.

#### References

- [1] W.M. Kays, A.L. London, Compact Heat Exchangers, McGraw-Hill, 1964.
- [2] G. Sun, Y. Li, Y. Lu, B. Khan, G.S. Tompa, Investigation of efficiency improvement on silicon solar cells due to porous layers, in: Materials Research Society Symposium—Proceedings, vol. 358, Microcrystalline and Nanocrystalline Semiconductors, 1995, pp. 593–598.
- [3] L. Urieli, D.M. Berchowitz, Stirling Cycle Engine Analysis, Adam Hilger Ltd., Bristol, Great Britain, 1984.
- [4] C.H. Chao, J.M. Li, Foam-metal heat sinks for thermal enhanced BGA package applications, in: The Eleventh International Symposium on Transport Phenomena ISTEP-II, Hsinchu, Taiwan, 1998, No. 4, pp. 23–29.
- [5] Y.C. Lee, W. Zhang, H. Xie, R.L. Mahajan, Cooling of a FCHIP package with 100 W, 1 cm<sup>2</sup> chip Proceedings of the ASME International Electron Package Conference, vol. 1, ASME, New York, 1993, pp. 419–423.
- [6] A.N. Pestryakov, A.A. Fyodorov, V.A. Shurov, M.S. Gaisinovich, I.V. Fyodorov, Foam metal catalysts with intermediate support for deep oxidation of hydrocarbons, React. Kinet. Catal. Lett. 53 (2) (1994) 347–352.
- [7] J.C. Armour, J.N. Cannon, Fluid flow through woven screens, AIChE J. 14 (3) (1968) 415–420.
- [8] J.R. Sodré, J.A.R. Parise, Friction factor determination for flow through finite wire-mesh woven-screen matrices, J. Fluids Eng. 119 (1997) 847–851.
- [9] S. Ergun, Fluid flow through packed columns, Chem. Eng. Prog. 48 (1952) 89–94.

- [10] D.P. Jones, H. Krier, Gas flow resistance measurements through packed beds at high Reynolds numbers, *J. Fluids Eng.* 105 (1983) 168–173.
- [11] D. Mehta, M.C. Hawley, Wall effect in packed columns, *I & EC Process Des. Develop.* 8 (2) (1969) 280–282.
- [12] R.P. Benedict, *Fundamentals of Temperature, Pressure, and Flow Measurements*, John Wiley & Sons, 1984.
- [13] S.J. Kline, F.A. McClintock, Describing the uncertainties in single-sample experiments, *Mech. Eng. (Am. Soc. Mech. Eng.)* 75 (1953) 3–8.
- [14] J.F. Liu, W.T. Wu, W.C. Chiu, W.H. Hsieh, Measurement and correlation of friction characteristic of flow through foam matrixes, *Experimental Thermal and Fluid Science*, submitted for publication.